JOURNAL OF GUIDANCE, CONTROL, AND DYNAMICS
Vol. 31, No. 5, September–October 2008

Selection of Rotorcraft Models for Application to Optimal Control Problems

Chang-Joo Kim,* Sang Kyung Sung,† Soo Hyung Park,‡ and Sung-Nam Jung§
Konkuk University, Seoul 143-70, Republic of Korea
and
Kwanjung Yee¶
Busan National University, Busan 609-735, Republic of Korea

DOI: 10.2514/1.33212

The maneuver characteristics of rotorcraft are analyzed using a nonlinear optimal control theory. The flight path deviations from a prescribed maneuver trajectory are penalized in the optimal control formulation to avoid numerical difficulties. The system optimality is represented by a two-point boundary value problem and solved via a multiple-shooting method. The focus of this paper is on the model-selection strategies for resolving the problems of numerical instability and high computational overhead when complex rotor dynamics are included in the mathematical model. Four different types of rotorcraft models are identified, two of which are linear models with or without rotor dynamics, as well as two models that include nonlinear dynamics for the rotor in its formulation. The effect each model was found to impart on the numerical analysis is reported. The relative computational efficiency is assessed in terms of computation time and the number of function calls for each model. The applications encompass the analyses for bob-up, turn, and slalom maneuvers and the results are used as guidelines for the selection of appropriate rotorcraft models.

Nomenclature

C_ψ, S_ψ	=	abbreviations of trigonometric functions cos ψ, sin ψ
F	=	jumps at shooting nodes
f	=	system forcing function
f_{CO}	=	total operating cost function ($f_{\mathrm{OP}} + f_{\mathrm{SC}}$)
f_{OP}	=	operating cost function
f_{SC}	=	penalty cost function for state constraints
g	=	forcing function vector for state variables
H	=	Hamiltonian
J	=	cost function
M	=	Jacobian matrix of F
p, q, r	=	angular velocity of the rigid body
Q, R	=	state and control weighting matrix
r	=	rotor radial position or residual in boundary conditions at initial time, shooting nodes, and final time
s	=	function for state constraints
U	=	feasible set of controls
u	=	control vector or longitudinal linear velocity
v, w	=	linear velocity in the y and z directions
x	=	state vector or x position
x_{CO}	=	state corresponding to cost function
x_E, y_N, h	=	x, y positions and altitude
y, z	=	state vectors, used in control formulation
Z	=	state and costate variables at shooting nodes
α	=	relaxation factor for Newton method
β	=	blade flap angle
δ	=	main rotor and tail rotor controls
λ	=	costate variables or inflow ratio
μ	=	Lagrange multipliers for terminal conditions
ϕ, θ	=	roll angle and pitch
φ	=	terminal cost function
ψ	=	yaw angle or function for terminal conditions

Subscripts

F	=	main rotor flap state
I	=	inflow state
R	=	rigid-body state
TR	=	tail rotor
trim	=	trim condition
0, 1C, 1S	=	collective, first cos, and first sin components

Received 3 July 2007; revision received 25 March 2008; accepted for publication 26 March 2008.

*Assistant Professor, Aerospace Information Systems Engineering, Hwayang-Dong, Gwangjin-Gu.
†Assistant Professor, Aerospace Information Systems Engineering, Hwayang-Dong, Gwangjin-Gu.
‡Assistant Professor, Aerospace Information Systems Engineering, Hwayang-Dong, Gwangjin-Gu. Member AIAA.
§Professor, Aerospace Information Systems Engineering, Hwayang-Dong, Gwangjin-Gu. Senior Member AIAA.
¶Assistant Professor, Aerospace Engineering, Jangjeon-Dong, Geumjung-Gu. Member AIAA.

I. Introduction

THE understanding of vehicle flight characteristics is one of the most challenging problems and the natural concern in the domain of flight dynamics. Because the mission of the modern aircraft has become increasingly aggressive and precise, good maneuver characteristics act as mandatory elements of the handling qualities requirements. The ADS-33 [1] handling qualities requirements for military rotorcraft designates 23 different mission task elements (MTEs) to verify favorable maneuver capabilities. The verification method specified in ADS-33 is the piloted simulation during the design phase up to critical design review (CDR) and first flight readiness review (FFR). However, only extensive flight test provides the final assessment of good maneuver capabilities. The same procedures should be followed for the category A certification of transport rotorcraft vehicle [2] after one engine failure or for the demonstration of the safe autorotation maneuver after all engines becomes inoperative. Because the full range of the flight envelope is involved for these tests, the related flight trials are generally expensive and hazardous to both the pilot and the vehicle itself. To mitigate the associated risks, much research has been carried out to develop reliable numerical methods which allow quick and low-cost design iteration at early design

stages and to provide benchmark results to enhance the productivity of future flight tests. However, there still exist many open issues on the adequate selection of the analysis method and the rotorcraft mathematical model. Because the highly aggressive or critical maneuvers are often performed near the boundary of the rotorcraft operational flight envelope (OFE), the fidelity of rotorcraft models should be high enough to provide solutions preserving the required accuracy. Also, the analysis methods available today generally require high computation time, even with today's advanced computing machines, or may show numerical instability when applied to the complex nonlinear rotorcraft model.

Inverse simulation and the dynamic optimization have been established in the rotary-wing design community as the preferred methods for analyzing vehicle maneuvers. Inverse simulation finds controls that enable the rotorcraft to follow a prescribed flight path whose trajectory is given as a function of time. Various inverse simulation methods [3–7] have been developed in the past decade. The integration inverse method, first proposed by Hess and Gao [3], has enjoyed a strong following because of its low dependency on a model's structure. The possibility of numerical instability or oscillatory behavior occurring in the solutions, however, causes some difficulties in obtaining robust solutions with a high-fidelity rotorcraft model. The time scale separation method by Avanzini and Matties [4] and the optimization method by Celi [5] are examples of techniques that endeavor to eliminate numerical instabilities by relaxing the conditions related to exact trajectory following. Nonetheless, it appears that further investigation is required to improve the robustness of these more recent approaches.

Alternatively, dynamic optimization [8–11] attempts to find the controls, states, and possibly the final time minimizing a cost function, subject to state equations and to various other constraints. There exist two alternative strategies for attaining numerical solutions of a dynamic optimization problem [8]. The first is an indirect method in which calculus of variation is first applied to find the necessary conditions for minimizing the cost function. Subsequently, the problem is reduced to a two-point boundary value problem (TPBVP) in the infinite dimension and a suitable shooting method can be used to resolve it in the finite dimension [10–13]. The second set of strategies is the direct method [8,9], which uses discretized or parameterized state equations, constraint equations, and a cost function in the finite dimension. The ensuing nonlinear optimization problem becomes numerically solvable with any nonlinear programming (NLP) methods. Sometimes, the parameterization is carried out in prior only for control variables (in the parametric optimal control problem) and the resultant system becomes a NLP in the control parameter vector in which the system constraints like system ordinary differential equation (ODE) and boundary conditions can be resolved using the shooting algorithm [11,14].

It is imperative that a dynamic optimization algorithm be carefully selected; an ideal choice is the one with well-balanced characteristics, such as fast convergence speed, large convergence radius, flexibility, simplicity, small data storage requirement, high accuracy, etc. Direct methods have been favored for analyzing a general large-scale dynamic system because system constraints could be easily handled. The large convergence radius, a feature of the direct method that allows a converged optimal solution from a large range of different initial guesses, has also contributed to the popularity of this strategy. Nevertheless, a couple of drawbacks of the direct methods merit the consideration of the indirect methods or the combined direct–indirect method for rotorcraft applications. First, important system characteristics can be lost during the parameterization stage, especially when the coarse grid for a parameter vector is used. Second, if not monitored carefully, the direct methods have the tendency to produce prohibitively large systems of equations. Balancing the convergence rate with high-precision accuracy through discretization in fine grid is challenging, as both are competing attributes. Because the converged solution with the direct method generally shows some discrepancy with the system optimality, the grid refinement test is inevitable to confirm the recovery of optimality conditions.

The convergence radii of indirect methods tend to be much smaller than those of the direct methods because their solutions using shooting methods are rather sensitive to poor initial guesses of states and costates. Finding a set of good initial estimates is often almost impossible because the costate variables are not explicit in their physical meaning. However, the indirect method generally displays rapid convergence rates and extremely high precision in the neighborhood of the optimal trajectory. To use the advantages of both the direct and indirect methods, the combined direct–indirect method has been proposed [10,14]. In this method, the direct method is used to generate initial guesses for the indirect method. The resultant algorithm proves to be more robust than the indirect method, whose convergence is not always guaranteed, and the optimum solution can be obtained.

The selection of the rotorcraft mathematical model is another important area because the model should have enough fidelity to cover the flight regime of interest. The trajectory predicted with an oversimplified model can generate a large discrepancy with real flight data even though it generally provides a fast and robust optimal solution. However, only a few researchers have focused on these modeling issues, and the related numerical difficulties are not fully exploited. In conjunction with rotorcraft models, Padfield [15] classifies the rotor modeling requirements by their area of application and flight envelope ranges. According to this classification, the level 1 rotor model uses the simplified quasi-linear aerodynamic theory to derive a closed form expression for resultant aerodynamic forces, and moments and can be applicable well within OFE. The level 2 rotor model needs the numerical integration of aerodynamic loads to include nonlinear and sophisticated aerodynamic evaluations of wake, inflow, unsteady aerodynamics, dynamic stall, etc., and can provide accurate solutions of flight dynamics problem up to OFE. The most complex level 3 model, which is generally used in the modern comprehensive rotorcraft analysis programs, includes the modeling of blade elastic deformation.

It is no secret that comprehensive rotorcraft modeling is a valuable enabler for evaluating vehicle performance, vibration, loads, stability, controllability, etc. Nevertheless, its application to rotorcraft flight control is not straightforward and is mostly limited to the validation of the design results through simulation. Recent studies by Bottasso et al. [16,17] tried to show the possibility of applying comprehensive models to the maneuver analysis of rotorcraft. They proposed a way of incorporating high-fidelity models into rotorcraft maneuver analysis routines. In response to the difficulty in adapting modern comprehensive analysis codes to optimal rotorcraft control problems, they combined a multibody model with flight mechanics models to create a single algorithm named the multibody steering algorithm. The parameters in the flight mechanics models are iteratively modified through a parameter identification method to match the rotorcraft responses obtained from the multibody model. Because the multibody model is used only for forward flight simulation with the controls calculated via the flight mechanics models, the analysis can be executed with relatively low computational overhead. In addition, a model predictive control (MPC) is applied for the purpose of stabilizing the unstable modes of rotorcraft during the open-loop simulation with the multibody model. However, the true worth of the analysis can only be achieved if each part of the algorithm responsible for parameter identification, MPC, and model coupling work flawlessly together, and the model for the parameter identification should have high fidelity suitable to the aggressiveness level of flight maneuvers. Another attempt at applying a high-fidelity model to MPC is the work of Bogdanov and Wan [18]. In this study, a Flightlab model with 92 internal states was created. Most states, except the 6 degrees of freedom (DOF) rigid-body states, were treated as unobservable and uncontrollable states and were thus excluded during the calculation of optimal controls. The wait time required for the control horizon of 25 s on a 3.75-GHz Pentium machine ranged from 24 min to 34 h, depending on the level of algorithmic sophistication.

Most contemporary analyses of optimal rotorcraft control problems are thus carried out using simplified models (below level 1) and are supplemented by the flight simulation using either level 1 or

level 2 rotor models. As far as the authors know, the complex rotor dynamics are not directly implemented in any publications for optimal control problems. Therefore, it is our understanding there is still a large gap between the model fidelity requirement and its numerical implementation. The previous studies by the authors [19,20] followed the same line of research as previously described, but the compromise in selecting a rotorcraft model was inevitable to get tractable solutions of rotorcraft maneuver problems. As rotorcraft require highly aggressive and precise maneuvers over the course of their mission, only the high-fidelity models can provide key insights on rotorcraft maneuver characteristics. Therefore, any compromise in model selection is still a big drawback even though inevitable.

The work reported herein encompasses the mathematical formulation of an indirect dynamic optimization method with different levels of rotor model sophistication and their application to the solution of rotorcraft maneuver problems. The indirect method is noted for its efficiency and robustness, but the converged solution satisfies the system optimality condition. As previously pointed out, the combined direct–indirect method can be used to enhance the robustness of the numerical solution. To simplify the analysis procedure, this research focuses on attempting to resolve the following technical challenges when the indirect method is used. However, the issues related to rotorcraft mathematical models are generally applicable to other methods.

First of all, the handling of system constraints is one of the major focal points of dynamic optimization. In principle, the control constraints are easily implemented by solving the control equations derived from Pontryagin minimum principle, even though the related numerical solution becomes one of the most time-consuming routines in the indirect method. The trajectory constraints (state constraints) need prior knowledge of the optimal trajectory to define the subarcs for active state constraints. Along these active arcs, the dynamic optimization treats the active constraints as equality (or algebraic) constraints in its solution procedure. Such a requirement complicates the implementation of the indirect method because of the possible generation of jumps in costates and Hamiltonian. Also, there exists a basic difficulty in defining the rotorcraft trajectory to be used as active equality constraints when a high-fidelity model is used because it is highly dependent on the unsteady rotor motion equations. The unsteadiness in rotor aerodynamic forces and moments causes the time-varying behavior in all state variables. Therefore, the implementation of hard constraints for rotorcraft trajectory along the subarcs is nearly nonachievable. Even a simple trim kinematical relation can be met using the states averaged over one rotor revolution as in the harmonic balance method or the periodic trimming algorithm [21,22]. Handling the prescribed trajectory constraints as hard constraints generally causes surplus oscillation in controls and this tendency becomes more and more severe for high forward speed [23]. In response to this perceived obstacle, the present paper uses a quadratic cost function to penalize any deviation from the prescribed maneuver trajectory, thus avoiding the difficulty in handling state constraints. The heuristic finding of suitable penalty parameters can reduce the usefulness of this approach, but a linear model can be extensively used in the program development phase to define such parameters with low computational burden.

The second challenge associated with the indirect methods is related to convergence, more specifically, convergence speed and radius. As previously mentioned, the combined direct–indirect method can improve the robustness and numerical accuracy, but it adds complexity in code generation and needs more computer resources as well as additional effort for tuning the solution strategies. Alternatively, this paper suggests the combined use of both linear and nonlinear models for their application to the indirect method. An optimal control solution using a linearized model is not only straightforward to find, but also useful to provide good initial guesses for the indirect method using a high-fidelity model. Therefore, the goal here is to attain an improvement in the indirect method's convergence radius that is meaningful enough to facilitate the widespread applications of high-fidelity models in identifying accurate flight characteristics over larger flight envelopes.

Lastly, the issue of system stability, which is especially important for an inherently unstable system like rotorcraft, is addressed. In general, time integration over a relatively large shooting segment leads to catastrophic results for the unstable system and this is a main reason why the single-shooting method (SSM) generally fails to get a converged solution for such system. Also, the size of a shooting segment in the multiple-shooting method (MSM) must thus be small enough to get a converged solution. This motivated the authors to analyze the influence of the shooting segment size on convergence characteristics and computational burden with a TPBVP solver. During this investigation, the minimum number of shooting nodes to guarantee numerical convergence was also explored.

Leveraging upon previous research on the flight dynamic analysis using fully implicit form of the rotor model [21], four different models were defined, which were used to obtain optimal control solutions to various rotorcraft maneuvers. Using two linear models with or without rotor and inflow dynamics, solution parameters (control weights and penalty parameters) and the number of shooting nodes for convergence is determined for their application to the optimal control solution with nonlinear models. A nonlinear 6-DOF rigid-body model is derived using a rotor trim solution, which generates the rotor contribution of forces and moments in response to the given rigid-body states and control inputs. This model can exclude the effect of unsteadiness in rotor aerodynamic forces and moments with additional computation burden to solve rotor trim equations. Finally, a nonlinear 12-DOF model, which allots an additional 6 DOF to main rotor flap and inflow dynamics, can retain the fidelity level required for the solution of aggressive rotorcraft maneuver problems. Needless to say, an efficient numerical solution method will enhance the practicality of applying higher-fidelity models like level 3 rotor models to rotorcraft optimal control problems. However, it is the authors' judgment that the present type of 12-DOF model is an adequate selection to get tractable optimal solutions with today's available methodologies and high-end computing machines.

The remainder of this paper is structured as follows. Section II presents the Mayer form of a nonlinear optimal control problem and the definition of cost function. The numerical procedure of the MSM is reviewed next in Sec. III, followed by the definition of four different linear and nonlinear rotorcraft models in Sec. IV. The numerical results of applying our proposed method to bob-up, turn, and slalom maneuvers are presented in Sec. V. Finally, the major findings of this study are recapitulated in Sec. VI.

II. Optimal Control Formulation

A. Problem Statement for Optimal Control and Necessary Conditions

The formulation of a general optimal control problem is covered in numerous textbooks, such as Bryson and Ho [23], Kirk [24], and in various papers. Here, key concepts related to the present study are reviewed. The optimal control problem, which takes the following standard Bolza form, is to find states $x^*(t)$, controls $u^*(t)$, and possibly final time t_f^* that minimize a cost function $J(\cdot)$:

$$\min J(x,u,t) = \varphi[x(t_f)] + \int_{t_0}^{t_f} f_{\mathrm{OP}}[x(t),u(t),t]\,\mathrm{d}t \tag{1}$$

$$\begin{aligned}
\text{subject to } & \dot{x}(t) = f[x(t),u(t),t] \\
& s[x(t),t] \le 0 \\
& x_i(t_0) = x_{i0} \qquad i \in I \subset \{1,\ldots,n\} \\
& \psi[x(t_f),t_f] = 0 \qquad \psi \subseteq R^k \\
& u(t) \in U \subseteq R^m \qquad t \in [t_0,t_f]
\end{aligned} \tag{2}$$

The operating cost function f_{OP} usually includes the quadratic function of controls to minimize control effort. If optimal controls calculated with this type of cost function are well within their limits, the control constraints can be ignored. For the problems in which the control constraints are critical, the constrained optimization can be

Table 1 Diagonal components of the state-weighting matrix. The components are the same for all MTEs except 1) $q_q = 40$ for side step and 2) $q_{\dot{\psi}} = 400$, $q = 350$, $q_{yN} = 0$ for turn

q_u	q_v	q_w	q_p	q_q	$q_{\dot{\psi}}$
200	7.5	7.5	7.5	15	200
q_ϕ	q_θ	q_ψ	q_{xE}	q_{yN}	q_h
100	500	35	0	100	30

used to solve control equations based on Pontryagin minimum principle.

One of the challenging issues in dynamic optimization is the handling of state inequality constraint $s[x(t), t] \leq 0$. Unlike the direct methods that can easily incorporate these constraints as part of a NLP algorithm, an indirect method requires complicated and tedious manipulation of the constraint functions. In the case that the state inequality constraints are active at any time of interest, the costate variables and Hamiltonian can show jumps at each touching point. Therefore, the Newton–Rhapson method used in MSMs cannot be applied as is. One way to remedy this situation begins by identifying the active arcs on which the state constraints can be described as algebraic equality constraints. Subsequently, system optimality can be obtained by solving switching conditions and algebraic equations for active constraints [23] together with the equations for system optimality. The numerical procedure thus ends up being very complex, in addition to requiring prior information on the optimal trajectory, which is nearly impossible to know in advance for complex nonlinear systems. In addition, the high-fidelity rotorcraft model generates the unsteady aerodynamic forces and moments which cause the time-varying behavior in all state variables. Even a simple flight path constraint, such as a forward flight with constant speed and altitude, is not achievable using instantaneous state variables but realizable with the averaged states over a suitable rotational period of rotor as in the harmonic balance or periodic trim algorithms. Therefore, the treatment of flight path as a hard constraint along active subarcs is infeasible and can result in numerical divergence [22].

An alternative method to employing equality constraints is an approach based on penalty functions, which formulates the search for system optimality as an unconstrained optimal control problem. Initially, the logarithmic penalty function method [25] appears to be applicable because it is capable of precisely handling boundary constraints with the barrier function approach. However, the computational overhead required to evaluate a point near a constraint boundary can become prohibitive if an ODE solver is used with tight

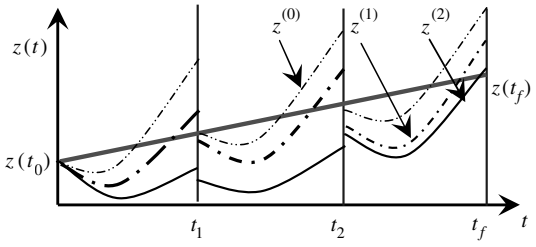

Fig. 1 Notional illustration of multiple-shooting method.

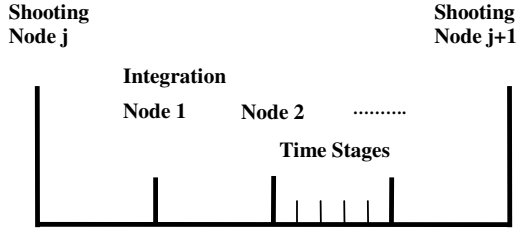

Fig. 2 Distribution of computational nodes.

Table 2 Descriptive parameters for rotorcraft maneuvers

Maneuver types	$(\Delta x)_{\max}$, m, deg	t_{entry}, s	t_{finish}, s
Bob up	$(\Delta h)_{\max} = 15$	2.0	8.0
Turn[a]	$(\Delta \psi)_{\max} = 90$	2.0	12.0
Slalom	$(\Delta y)_{\max} = 10$	1.0	9.0

[a] $t_{\text{steady}} = 5.0$ s and $t_{\text{exit}} = 9.0$ s for the turn maneuver.

step-size control. Another disadvantage of the logarithmic penalty function method is that further analysis is impossible if one of the constraints is violated over the course of time integration. The authors are aware that there is a high probability of such an occurrence when the MSM is applied to unstable systems. Consequently, it was decided to use a quadratic penalty function approach to trajectory deviations from a prescribed maneuver path. With the penalty cost f_{SC} for state constraints, the original optimal control formulation can be rewritten as the following optimal control problem in the standard Bolza form

$$\min J(x,u,t) = \varphi[x(t_f)] + \int_{t_0}^{t_f} f_{\text{OP}}[x(t),u(t),t] + f_{\text{SC}}[x(t),t]\,\mathrm{d}t \quad (3)$$

$$\begin{aligned} \text{subject to } & \dot{x}(t) = f[x(t),u(t),t] \\ & x_i(t_0) = x_{i0} \qquad i \in I \subset \{1,\ldots,n\} \\ & \psi[x(t_f),t_f] = 0 \\ & \psi \subseteq R^k \qquad t \in [t_0,t_f] \end{aligned}$$

This form of equations can be transformed into the Mayer form by defining the cost state x_{CO} and the corresponding initial condition as

$$\min J(x,u,t) = \varphi[x(t_f),t_f] + x_{\text{CO}}(t_f) \quad (4)$$

$$\begin{aligned} \text{subject to } & \dot{x}(t) = f[x(t),u(t),t] \\ & \dot{x}_{\text{CO}}(t) = f_{\text{CO}}[x(t),u(t),t] \\ & \qquad = f_{\text{OP}}[x(t),u(t),t] + f_{\text{SC}}[x(t),t] \\ & x_i(t_0) = x_{i0} \\ & x_{\text{CO}}(t_0) = 0 \\ & \psi[x(t_f),t_f] = 0 \end{aligned} \quad (5)$$

The first-order necessary condition for system optimality can be derived from applying calculus of variation to the cost function by adjoining system equations and boundary conditions. Based upon the formulation in [23,24], optimality conditions can be written as the following TPBVP with states $y(t) = [x(t), x_{\text{CO}}(t)]^T \in R^{n+1}$, costates $\lambda(t) \in R^{n+1}$, Lagrange multiplier $\mu(t) \in R^k$, and Hamiltonian $H = \lambda^T(t) g[y(t),u(t),t]$:

$$\dot{z}(t) = \begin{bmatrix} \dot{y}(t) \\ \dot{\lambda}(t) \\ \dot{\mu}(t) \end{bmatrix} = \begin{bmatrix} g(y(t),u(t),t) \\ -\{g_y(\cdot)\}^T \lambda(t) \\ 0 \end{bmatrix} \quad (6)$$

$$r[z(t_0),z(t_f)] = \begin{bmatrix} x_i(t_0) - x_{i0} \\ x_{\text{CO}}(t_0) \\ \psi(x(t_f),t_f) \\ \lambda(t_f) - \left(\frac{\partial(\varphi + x_{CO})}{\partial y}\right)^T_{t=t_f} - \left(\frac{\partial \psi}{\partial y}\right)^T_{t=t_f} \mu \end{bmatrix} = 0 \quad (7)$$

where the algebraic equations for optimal controls are

$$u^*(t) = \arg \min_u H(x^*,u,\lambda^*,t) \quad (8)$$

or

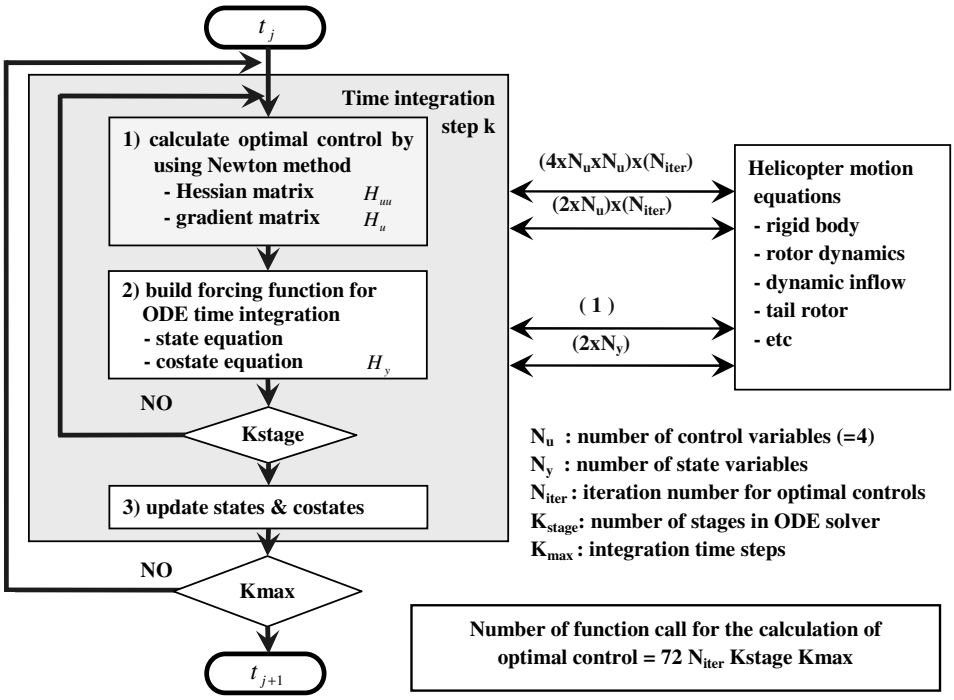

Fig. 3 Time-integration routine and number of function calls.

$$\frac{\partial H(x^*, u, \lambda^*, t)}{\partial u} = 0 \tag{9}$$

B. Description of Maneuver Trajectory

Trajectory generation has been an increasingly active research topic because of its usefulness as an aid to vehicle motion planners for the online guidance and control of autonomous air vehicles. High-level flight functions, such as obstacle avoidance and terrain following, etc., can be implemented with a trajectory generated in optimal ways. The successful implementation of such functions can be achieved through the combinations of various aggressive, three-dimensional maneuvers. Because the focus of this research is on the model-selection aspect of implementing optimal control problems, the authors opt to adapt a suitable trajectory prescription method, with minor modifications, rather than to create an entirely new approach. Representing a trajectory with polynomial and trigonometric functions is a widely used approach in inverse simulation studies of the rotorcraft because of its analytical simplicity and smoothness [6,7,26]. The feasibility of a generated trajectory can be further enhanced by correlating it with actual flight test results. In particular, the piecewise continuous polynomial approach by Thomson and Bradley [26] is very attractive because the method is capable of providing a simple yet effective way of modeling even the highly aggressive maneuvers. A trajectory generated by this method has been reported to agree well with flight test data in predicting the handling-quality requirements for roll quickness parameters [7]. Similar analytical descriptions as to those for inverse simulation were adapted for this study as follows.

The trajectory can be expressed as the sum of states at maneuver entry and its variation during the maneuver.

$$x(t) = x(t_{\text{entry}}) + \Delta x(t) \tag{10}$$

or

Table 3 System eigenvalues of four different models

M2 and M4 models using averaged state equation	M2 and M4 models using Floquet transition matrix	M3 model using averaged state equation	M1 model using reduced-order state equation
−0.966E − 01	−0.999E − 01	−0.102E + 00	−0.102E + 00
−0.157E + 00 + *i*0.399E − 01	−0.161E + 00 − *i*0.428E − 01	−0.299E + 00	−0.298E + 00
−0.157E + 00 − *i*0.399E − 01	−0.161E + 00 + *i*0.428E − 01	0.480E + 00 − *i*0.250E + 00	0.482E + 00 + *i*0.248E + 00
−0.369E + 00 + *i*0.133E + 00	−0.386E + 00 + *i*0.119E + 00	0.480E + 00 + *i*0.250E + 00	0.482E + 00 − *i*0.248E + 00
−0.369E + 00 − *i*0.133E + 00	−0.386E + 00 − *i*0.119E + 00	−0.414E + 00 − *i*0.194E + 01	−0.415E + 00 + *i*0.194E + 00
0.286E + 00 + *i*0.348E + 00	0.238E + 00 + *i*0.352E + 00	−0.414E + 00 + *i*0.194E + 01	−0.415E + 00 − *i*0.194E + 00
0.286E + 00 − *i*0.348E + 00	0.238E + 00 − *i*0.352E + 00	−0.354E + 01	−0.354E + 01
−0.385E + 00 + *i*0.197E + 01	−0.381E + 00 − *i*0.195E + 01	−0.101E + 02	−0.101E + 02
−0.385E + 00 − *i*0.197E + 01	−0.381E + 00 + *i*0.195E + 01	——	——
−0.652E + 01	−0.508E + 01	——	——
−0.136E + 02	−0.117E + 02 + *i*0.687E + 01	——	——
−0.103E + 02 + *i*0.903E + 01	−0.117E + 02 − *i*0.687E + 01	——	——
−0.103E + 02 − *i*0.903E + 01	−0.168E + 02	——	——
−0.181E + 02 + *i*0.464E + 02	−0.203E + 02 + *i*0.443E + 02	——	——
−0.181E + 02 − *i*0.464E + 02	−0.203E + 02 − *i*0.443E + 02	——	——
−0.186E + 02 + *i*0.463E + 02	−0.210E + 02 + *i*0.451E + 02	——	——
−0.186E + 02 − *i*0.463E + 02	−0.210E + 02 − *i*0.451E + 02	——	——
−0.180E + 02 + *i*0.902E + 02	−0.203E + 02 + *i*0.881E + 02	——	——
−0.180E + 02 − *i*0.902E + 02	−0.203E + 02 − *i*0.881E + 02	——	——

$$x(t) = x(t_{\text{entry}}) + \int_{t_{\text{entry}}}^{t} \Delta\dot{x}(\tau)\,\mathrm{d}\tau \tag{11}$$

Trigonometric functions are good basis functions for trajectory generation [6] because of their intrinsic smoothness. For this study, the height variations of bob-up maneuvers and the lateral position changes of slalom maneuvers are described with Eqs. (12) and (13), respectively. The terms t_{entry} and t_{finish} designate maneuver entry and finish times, where $(\Delta x)_{\max}$ is the maximum change in a state variable during maneuver in terms of altitude, heading, and speed, etc.

$$\Delta x(\bar{t}) = \frac{(\Delta x)_{\max}}{16.0}[8 + \cos(3\pi\bar{t}) - 9\cos(\pi\bar{t})] \tag{12}$$

$$\Delta x(\bar{t}) = \frac{(\Delta x)_{\max}}{46.8}[32 + \sin(2\pi\bar{t}) - 20\sin(4\pi\bar{t}) + 2\sin(8\pi\bar{t})] \tag{13}$$

where

$$\bar{t} = (t - t_{\text{entry}})/(t_{\text{finish}} - t_{\text{entry}}) 0 \le \bar{t} \le 1$$

A typical maneuver can be described in terms of different maneuver phases, such as entry stage, steady maneuver phase, and exit phase. The piecewise polynomial method proposed by Thomson and Bradley [26] is well suited for the generation of trajectories corresponding to each maneuver phase. By changing the time required for the entry phase and/or the exit phase, the level of maneuver aggressiveness can be controlled. A turning flight with a constant turn rate is an example of a steady maneuver phase. The flight direction angle for a turn maneuver is accordingly defined with the following mathematical formulation, yielding:

$$\Delta\dot{x}(t) = \begin{cases} (\Delta\dot{x})_{\max}(-2\bar{t}^3 + 3\bar{t}^2), & t_{\text{entry}} \le t \le t_{\text{steady}} \\ (\Delta\dot{x})_{\max}, & t_{\text{steady}} \le t \le t_{\text{exit}} \\ (\Delta\dot{x})_{\max}(-2\tilde{t}^3 + 3\tilde{t}^2), & t_{\text{exit}} \le t \le t_{\text{finish}} \end{cases} \tag{14}$$

$$\begin{aligned} (\Delta\dot{x})_{\max} &= (\Delta x)_{\max}/(t_{\text{finish}} + t_{\text{exit}} - t_{\text{steady}} - t_{\text{entry}}) \\ \bar{t} &= (t - t_{\text{entry}})/(t_{\text{steady}} - t_{\text{entry}}) \\ \tilde{t} &= 1 - (t - t_{\text{exit}})/(t_{\text{finish}} - t_{\text{exit}}) \end{aligned} \tag{15}$$

The maximum steady turn rate $(\Delta\dot{\psi})_{\max}$ and the maximum angular acceleration $(\Delta\ddot{\psi})_{\max}$ can be easily adjusted as per the required input parameters such as $(\Delta\psi)_{\max}$, t_{steady}, t_{entry}, t_{finish}, and t_{exit}.

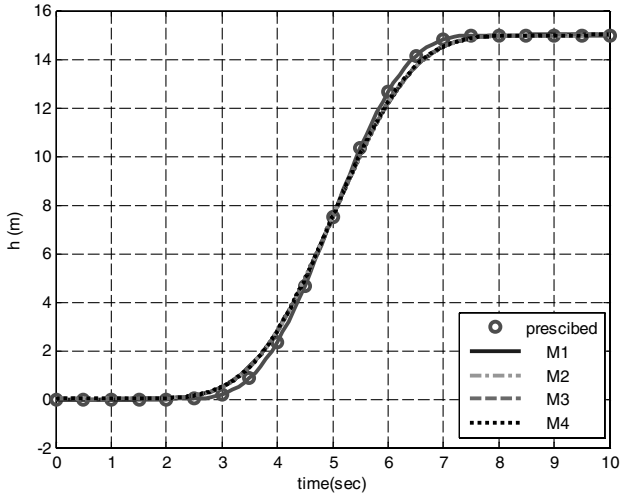

Fig. 4 Height variation during bob-up maneuver with different models.

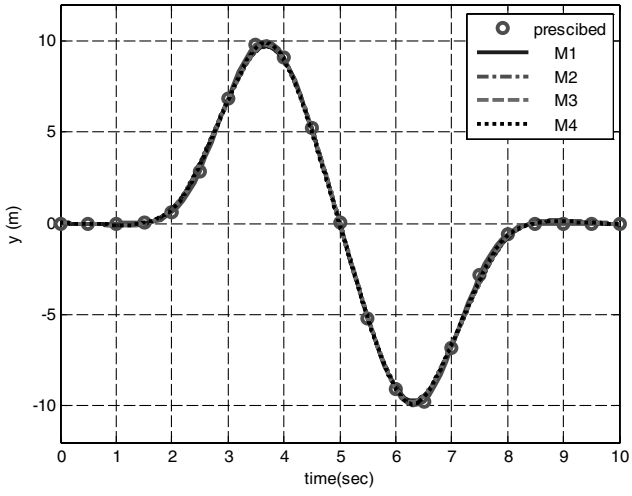

Fig. 5 *Y*-position change during slalom maneuver with different helicopter models.

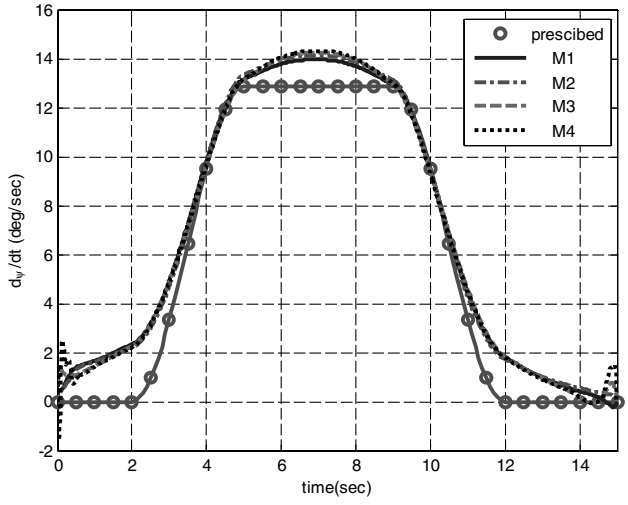

a) Heading angular rate

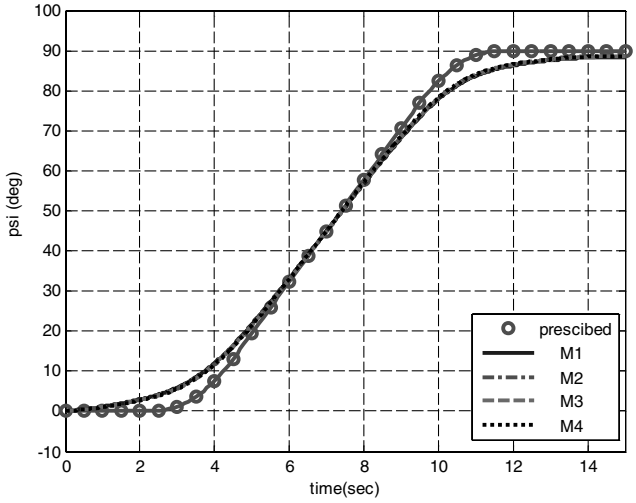

b) Heading angle

Fig. 6 Time history of heading angle and heading rate at turn maneuver with different models.

Because a vehicle's maneuver is carried out in a three-dimensional space, it is necessary to define it in terms of all three axes. Most maneuvers, defined in modern handling-quality requirements such as ADS-33 [1], begin from a stabilized trim condition and terminate with another steady flight condition. The requirements for maneuver accuracy are commonly specified in terms of bounded deviations from stabilized trim reference parameters, such as flight speed, altitude, sideslip, heading, positions, etc. The same quantities were used in a similar manner in the present study for describing the reference trajectory for other axes. Table 2 lists parameters in this paper for bob-up, turn, and slalom maneuvers.

C. Cost Function and Boundary Conditions

As previously mentioned, the numerical implementation of a state constraint is quite difficult with the indirect method. Therefore, the state constraints in this study are modeled with the quadratic penalty function:

$$f_{\mathrm{CO}}(\bar{x}_R(t), u(t), t) = 0.5(\bar{x}_R - \bar{x}_{\mathrm{target}})^T Q(\bar{x}_R - \bar{x}_{\mathrm{target}}) + 0.5(u - u_{\mathrm{trim}})^T R(u - u_{\mathrm{trim}}) \tag{16}$$

where

$\bar{x}_R$: reduced rigid body states $\quad \bar{x}_{\mathrm{target}}$: target states

$$\bar{x}_R(t) = [u, v, w, p, q, \dot{\psi}, \phi, \theta, \psi, x_E, y_N, h]^T$$

$$R = \mathrm{diag}(r_{\delta_0}, r_{\delta_{1C}}, r_{\delta_{1S}}, r_{\delta_{\mathrm{TR}}})$$

$$Q = \mathrm{diag}(q_u, q_v, q_w, q_p, q_q, q_{\dot{\psi}}, q_\phi, q_\theta, q_\psi, q_{xE}, q_{yN}, q_H)$$

The target states $\bar{x}_{\mathrm{target}}(t)$ are set to be the trim states $(x_R)_{\mathrm{trim}}$, except those that need the description of their time variation for a specific maneuver. The same control weighting matrix R is used throughout this paper with its diagonal components as

$$r_{\delta_0} = 3600, \qquad r_{\delta_{1C}} = 900, \qquad r_{\delta_{1S}} = 900, \qquad r_{\delta_{\mathrm{TR}}} = 600 \tag{17}$$

The positive semidefinite weighting matrix Q for tracking errors consists of components listed in Table 1. The components show small variations in their values, depending on the required tracking accuracy for a specific maneuver.

The initial conditions for the state variables are specified with the results of trim analysis because all maneuvers considered for this study are initiated from a steady trim condition with their terminal conditions defined in terms of the target states at the end of a maneuver:

$$x_i(t_0) = x_{i,\ \mathrm{trim}} \qquad i = 1, \ldots, n, \qquad \bar{x}(t_f) = \bar{x}_{\mathrm{target}}(t_f) \tag{18}$$

Because the penalized cost function already accounts for the same conditions, the implementation of the terminal constraints can be used for both 1) the exact matching of our trajectory with a target trajectory at the final time and 2) leading to an improved convergence behavior of the MSM. The terminal cost function can be set to zero if time-optimal problems are excluded.

III. Numerical Methods

The shooting algorithm [10,12,13] is a commonly used method for solving a TPBVP in ordinary differential equations. Because the application of a SSM [27] to unstable systems like rotorcraft is found to result in divergence, the discussion that follows is focused on the MSM. The MSM refers to the discretization of a trajectory into a number of subintervals, each of which contains a separately defined initial value problem. Successive iterations follow until both the boundary conditions and the continuity of the state variables at each subinterval node are satisfied. Figure 1 illustrates one such MSM procedure. This study follows the procedure of the BNDSCO (a program for the numerical solution of optimal control problems) software developed by Oberle and Grimm [13] to solve optimal control problems with state equality and/or inequality constraints. The nomenclature convention of [13] is used to describe this

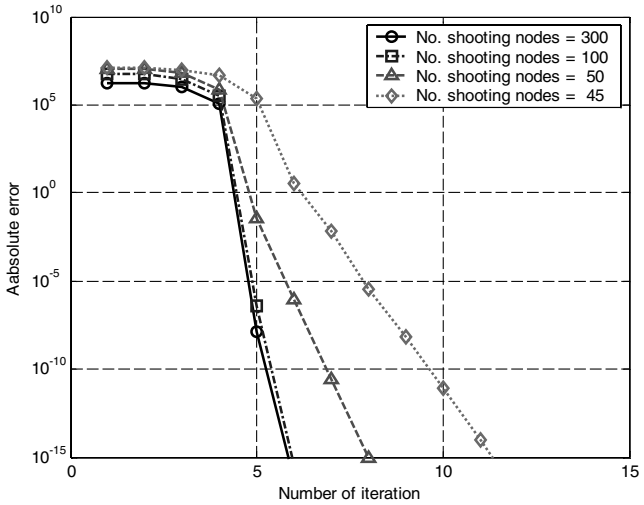

Fig. 7 Convergence history of MSM for bob-up maneuver (effect of the number of shooting nodes: M1-NI6).

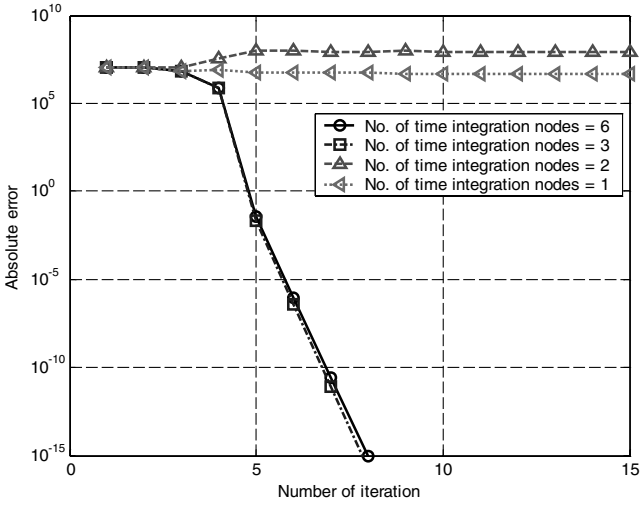

Fig. 8 MSM convergence history for bob-up maneuver (effect of the number of time-integration nodes: M1-NS50).

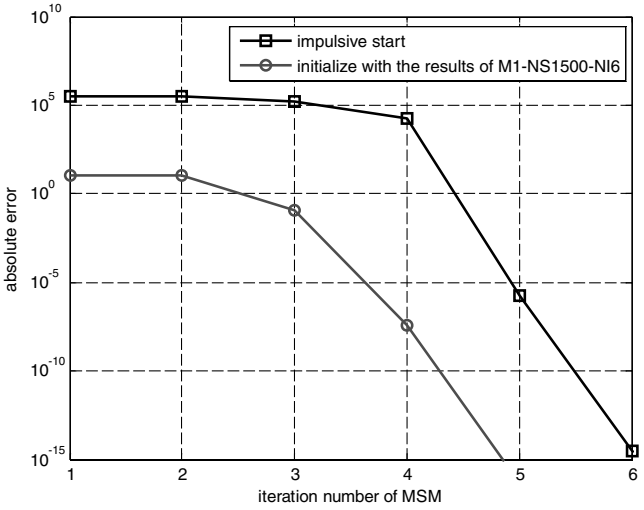

Fig. 9 Effect of initialization methods on convergence history (bob-up maneuver, M3-NS1500-NI6).

numerical procedure. First, the time domain $[t_0, t_f]$ is divided into multiple subintervals to define the time nodes for multiple shooting. Next, an iterative procedure consisting of the following steps is implemented:

1) Define $(m+1)$ shooting nodes $t_0 := t_1 < t_2 < \cdots < t_m := t_f$.

2) Guess initial values of $z(t_j)$ with $Z_j^{(0)}$, $j = 1, 2, \ldots, m$.

3) Iteratively solve TPBVP.

Step 1: Integrate ODE over each subinterval to find the integrated value of z at time t with an initial condition $z(t_j) = Z_j$ as $z(t) = z(t; t_j, Z_j) t_j \le t \le t_{j+1}$.

Step 2: Compute jumps F_j at each shooting node $(1 \le j \le m-2)$ $F_j(Z_1, Z_2, \ldots, Z_{m-1}) := z(t_{j+1}; t_j, Z_j) - Z_{j+1}$ and evaluate the residual in the boundary conditions $F_{m-1}(Z_1, Z_2, \ldots, Z_{m-1}) := r(Z_1, Z_{m-1})$.

Step 3: Calculate an approximate Jacobian matrix M of $F(Z_1, Z_2, \ldots, Z_{m-1})$.

Step 4: Solve the matrix equation to find the corrections ΔZ for states and costates $M\Delta Z = -F(Z_1, Z_2, \ldots, Z_{m-1})$.

Step 5: Update the state and costate variables $Z^{\text{new}} = Z + \alpha \Delta Z$ $\alpha \in [0, 1]$.

Figure 2 presents the distribution of computational nodes between two adjacent shooting nodes, which include the time-integration nodes and time stages for a multistage ODE solver. The time-integration routine in step 1 and step 3 is the innermost part of the iterative MSM, and the computation time of this routine determines the overall efficiency of the numerical analysis. For the time integration, a nonlinear algebraic equation, Eq. (8) or Eq. (9), must be solved to obtain the optimal controls. Figure 3 shows the time-integration procedure from shooting nodes t_j to t_{j+1} including the optimal control calculation routine. The number of function calls to calculate $\dot{y}(t) = g[y(t), u(t), t]$ is estimated when the optimal control equations are iteratively solved with the standard Newton–Rhapson method, and the related Hessian matrix H_{uu} and gradient vector H_u are approximated with the central difference formula. As an example, with $N_{\text{iter}} = 10$, $N_u = 4$, and $N_y = 22$ (12 states for rigid-body states, 3 states for dynamic inflow, 6 states for main rotor flap motions, and one state for cost function), the total number of function calls become the sum of 720 (for the calculation of optimal controls) and 45 (for the forcing functions of state and costate equations). The number of function calls required for one-step integration is around 765 times greater than that for forward simulation. Such a need for additional number of outer MSM iterations provides motivation to seek ways to meaningfully reduce the wait time, even in today's high-speed computing environments, and especially when a high-fidelity mathematical model is desired.

The most time-consuming routine of the optimal control calculation is the evaluation of the Hessian matrix H_{uu}. If an optimal control is obtained by solving Eq. (9) with an efficient NLP approach using first-order methods, rather than Eq. (8) with the Newton–Rhapson method, it is possible to avoid the explicit calculation of the full Hessian matrix because the efficient NLP requires only the first-order gradient information. Additionally, the implementation of the control constraints is straightforward in a NLP algorithm. Although the first-order methods are suitable for the resolution of typical nonlinear programming problems, they usually need much iteration or fail to find the optimal controls with high enough accuracy to be used in the succeeding forward simulation. The differential algebraic equation (DAE) approach can be used to simultaneously solve both

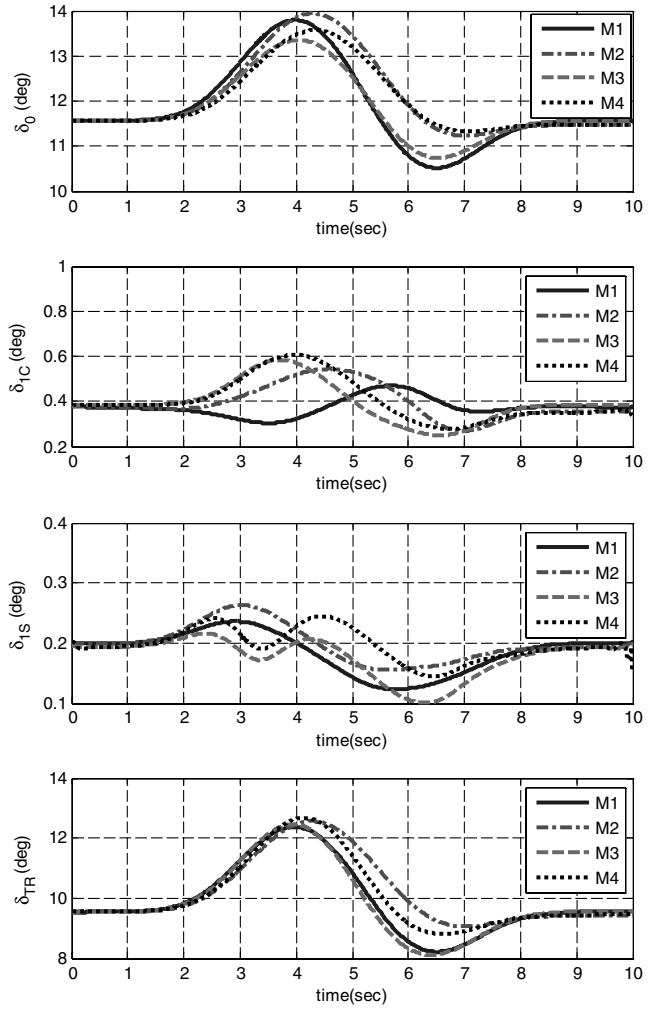

Fig. 10 Time history of optimal controls for bob-up maneuver (NS1500-NI6).

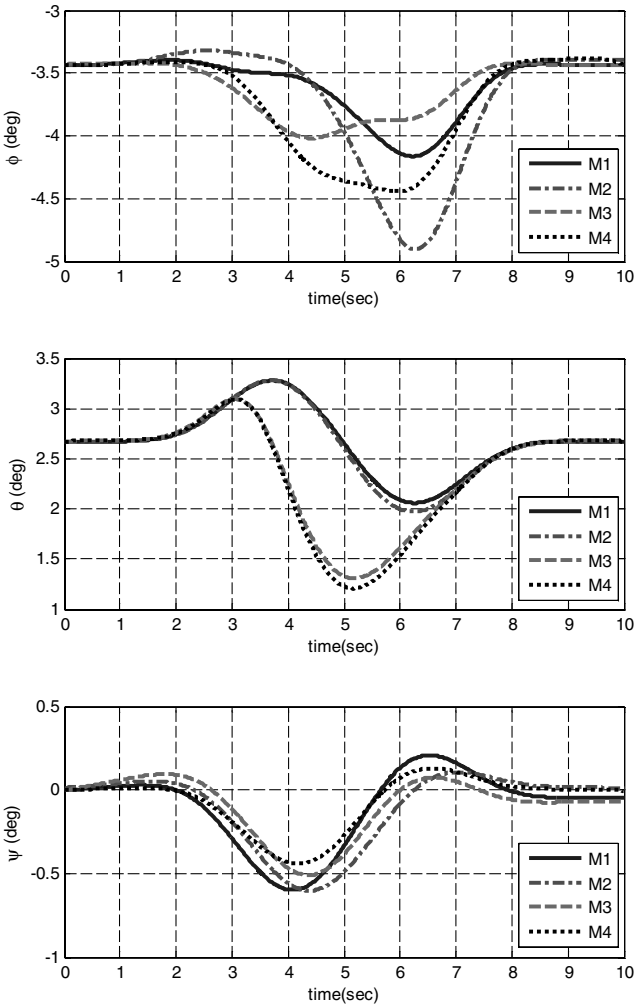

Fig. 11 Time history of attitude and heading angle for bob-up maneuver (NS1500-NI6).

the ordinary differential Eq. (6) and the algebraic Eq. (8). Because a MSM numerically calculates an approximate Jacobean matrix M of $F(Z_1, Z_2, \ldots, Z_{m-1})$ by perturbing the system's initial states one at a time at each shooting node, the computation of consistent initial conditions at every time step can reduce the efficiency of DAE solvers [22]. Moreover, a tight step-size control, which is usually adopted in general DAE solvers, is likely to not only increase the number of function calls, but also to fail to continue the time integration when a calculated step size is less than the specified step-size tolerance. Because of the high-frequency modes found in rotor dynamics, the occurrence of this situation is highly probable in the optimal control problem of rotorcrafts.

If system equations are affine in controls and a quadratic cost function is used for control effort with positive definite weighting matrix R as

$$\text{affine system}: \dot{x}(t) = f_1[x(t), t]u(t) + f_2[x(t), t] \tag{19}$$

$$\text{cost for control}: \int_{t_0}^{t_1} 0.5(u - u_{\text{trim}})^T R(u - u_{\text{trim}})\, \mathrm{d}t \tag{20}$$

then, from a modeling perspective, the Hessian H_{uu} can be approximated with $\lambda_{\text{CO}}R$, requiring no further function calls. It can also be a good approximation for the system nearly affine in controls, which is the typical case even for nonlinear rotor dynamic equations. This kind of Hessian approximation is used in the present study and presents the same convergence character as the solution using the numerical estimation of the full Hessian matrix. Also, the gradient vectors H_y and H_u are numerically calculated by using a central difference formula. In addition, the computational overhead for estimating these gradient vectors is reduced by considering the dependency of the vector components of the forcing function $g[y(t), u(t), t]$ in Eq. (6) on the control and state variables. A four-stage Runge–Kutta algorithm with a constant time-step size was used throughout this study, and the required time-integration accuracy was endeavored to be satisfied by adjusting the number of shooting nodes as well as the number of time steps.

IV. Rotorcraft Mathematical Models for Flight-Maneuver Analysis

The helicopter flight dynamics models used in this study are based on previous work [21], which describes the formulation of rotor dynamic equations for flap, lead lag, and RPM dynamics in fully implicit form. The rotor system is modeled with rigid blades attached to the hub through a sequence of hinges with equivalent springs and dampers. Nonlinear quasi-steady aerodynamic theory is applied through a table look-up procedure. If the main rotor dynamics are described only with flapping, then the resultant system of flight dynamics equations can be partitioned into rigid-body motion, flap motion, inflow dynamics, and tail rotor as follows:

$$f(\dot{x}, x, u, t) = [f_R,\ f_F,\ f_I,\ f_T]^T = 0 \tag{21}$$

$$x = [x_R,\ x_F,\ x_I,\ x_T]^T \tag{22}$$

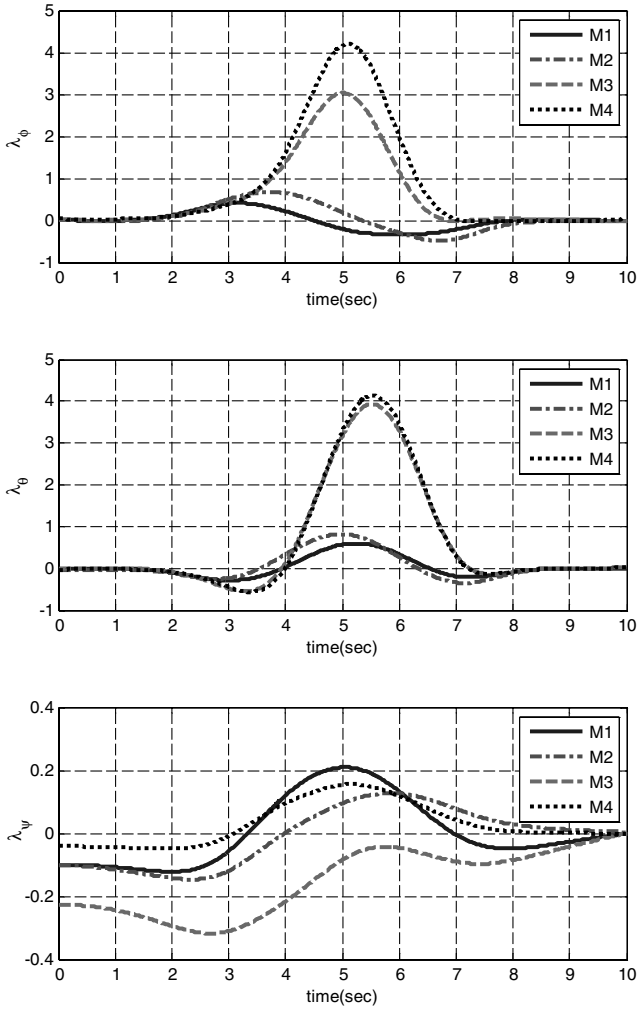

Fig. 12 Time history of costates corresponding to attitudes and heading angle for bob-up maneuver (NS1500-NI6).

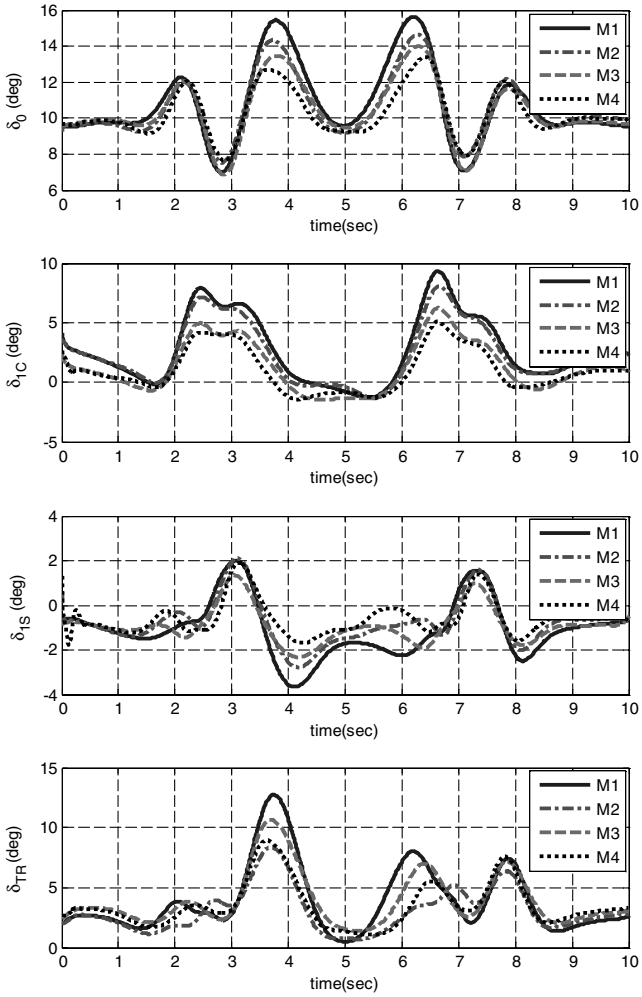

Fig. 13 Time history of optimal controls for slalom maneuver (NS1500-NI6).

$$x_R = [u, v, w, p, q, r, \phi, \phi, \theta]^T$$
$$x_F = [\dot{\beta}^{(1)}, \dot{\beta}^{(2)}, \dot{\beta}^{(3)}, \dot{\beta}^{(4)}, \beta^{(1)}, \beta^{(2)}, \beta^{(3)}, \beta^{(4)}]^T \quad (23)$$
$$x_I = [\lambda_o, \lambda_{1C}, \lambda_{1S}]^T \qquad x_T = [\beta_{\mathrm{TR1}C}, \beta_{\mathrm{TR1}S}, \lambda_{\mathrm{TR0}}]^T$$

where x_R, x_F, x_I, and x_T are the state variables for airframe rigid-body motion, main rotor flap of individual blades, dynamic inflow, and tail rotor, respectively. The dynamic equations of rotorcraft motion described here become the system of implicit differential algebraic equations. The control inputs for main rotor collective pitch, lateral cyclic pitch, longitudinal cyclic pitch, and tail rotor control are defined as

$$u = [\delta_0, \delta_{1C}, \delta_{1S}, \delta_{TR}]^T \quad (24)$$

For trim analysis, two different methods were investigated. One was a harmonic balance method which represents blade flap angles in hub-fixed coordinates through multiblade coordinates (MBCs) transformation. The other was a periodic trim algorithm using individual blade flap angles to find the initial states that meet the periodic trim conditions with constant controls. Flight stability can be judged by analyzing the eigenvalues of a linear state equation derived at a calculated trim condition or by applying the Floquet stability theory to a state transition matrix obtained during the periodic trim calculation. DAE solvers were employed for time integration in the periodic trim routine. Further details on the modeling and simulation aspects of our flight dynamic equations are found in [21]. The direct application of the motion equations such as Eq. (21) to rotorcraft optimal control problems is not trivial because of the time-varying nature of state variables and the high computational overhead for numerically integrating aerodynamic forces and moments over the radial positions of individual blades. In response to these challenges, the present study investigates the impact of the different levels of model fidelity on the optimal solution quality, which can provide objective guidelines for selecting a suitable model for a given rotorcraft flight dynamics problem.

It is widely accepted that a level 2 rotor model [15] is a proper choice for the analysis of flight maneuvers. Such a model contains the blade element method, whereby the distribution of air loads along the blade span is numerically integrated over all blades to obtain the aerodynamic forces and moments generated by the entire rotor system. Logically, the use of rotor motion states defined in the rotating individual blade coordinate system, as in Eq. (21), would be recommended here. From a practical point of view, however, the use of motion variables, such as the individual blade flap states, hinder the convergence to system optimality due to the time-varying nature of system states. For instance, the calculation results of rotorcraft periodic trim with aeromechanically similar blades would always display an oscillatory behavior in the trim state variables, including those representing rigid-body states. Such a tendency complicates the task of forming consistent initial guesses for the stable operation with the MSM. Even a small phase shift in the oscillatory rotorcraft response can cause an erroneous estimation of the Hamiltonian gradients (H_u and H_x), causing the iterative MSM to fail to converge.

Algebraic or even first-order ODE equations for tip path plane tilt are commonly used for modeling rotor dynamics because such models use a closed-form expression for rotor aerodynamic forces and moments, thus relieving the burden on local computational resources. The high-frequency modes of rotor motion are also customarily excluded with the simple dynamical models, allowing

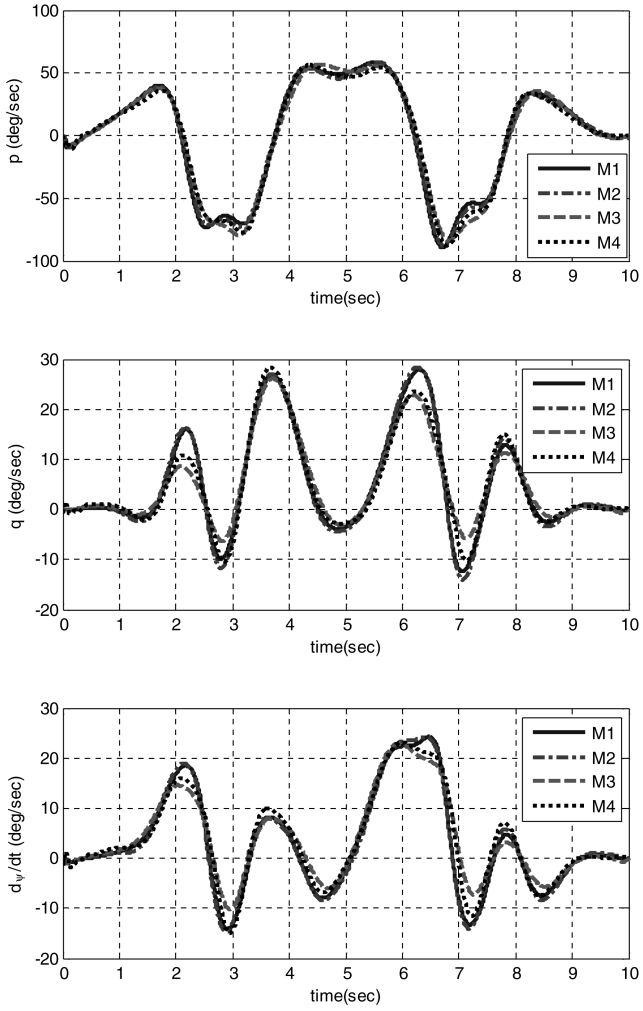

Fig. 14 Time history of attitude and heading rate for slalom maneuver (NS1500-NI6).

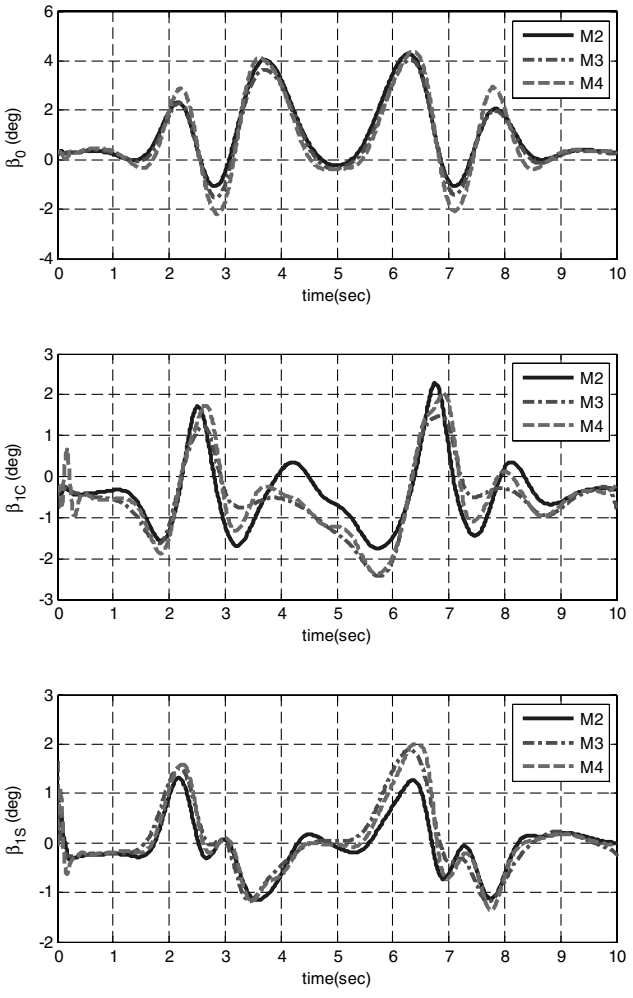

Fig. 15 Time history of flap angle for slalom maneuver (NS1500-NI6).

the system of equations to be integrated with sparsely distributed time steps.

The level 2 rotor model, such as Eq. (21), can be described with flap variables defined in the hub-fixed coordinate system through the use of MBCs transformation. The classical approach by Chen [28] used hub-fixed flap states to derive the closed form expression for aerodynamic forces and moments based on quasi-linear aerodynamic theory. Still, higher harmonic terms are not completely omitted, potentially leading to the same kind of adverse effect individual blade flap states exert on the convergence behavior toward an optimal control solution. The tip path plane dynamics are commonly used to remove these higher harmonic terms, in which the flap motions are approximated by first-harmonic components with time-varying coefficients only. The resultant equations of motion possess no higher harmonic terms and the equations for the tip path plane dynamics are in the form of second-order ODEs.

Chen's [28] approach is a classic example of how the competing desires for both reasonable wait time and good convergence led to a compromise in modeling fidelity. A further reduced-order model for tip path plane dynamics has been shown to exhibit even higher solution efficiency according to [28], which has demonstrated its validity within the low frequency range of rotorcraft flight simulations. Nonetheless, the importance and advantages of employing a higher-fidelity rotor model cannot be emphasized enough and should be pursued in the advent of new computer technology or new algorithms for robust optimal control analysis.

To reiterate, the helicopter flight dynamics equations used for the present study are modified versions of those reported in [21]. All component models are identical except the one corresponding to the main rotor. In an effort to remove the higher harmonic components in the main rotor equation for flapping motions, aerodynamic forces, and aerodynamic moments, quasi-linear aerodynamic theory is applied to the calculation of sectional aerodynamic forces as

$$dF_X^{\text{aero}} = \frac{1}{2} C_{L\alpha} \rho \left[\theta U_T U_P - U_P^2 + \left\{ \frac{c_{d0} + c_{d2} C_T^2}{C_{L\alpha}} \right\} (U_T^2 + U_P^2) \right] c dr$$

$$dF_Z^{\text{aero}} = \frac{1}{2} C_{L\alpha} \rho \left[\theta (U_T^2 + U_P^2) - \left\{ 1 + \frac{c_{d0} + c_{d2} C_T^2}{C_{L\alpha}} \right\} U_T U_P \right] c dr \tag{25}$$

The sectional aerodynamic forces in blade flap coordinate system F_X^{aero} and dF_Z^{aero} are in-plane and normal components, respectively. The present derivation of main rotor modeling equations differs from the classical approach by [28] in that: 1) no ordering scheme is applied to simplify the final derivation, and 2) it includes all nonlinear terms related to rigid-body states as well as gravitational acceleration.

The linear model used in this study is derived from the helicopter motion equations of Eq. (21) in time invariant form. The trim solutions are computed with the harmonic balance method, and the perturbed motion equations are numerically derived at each azimuth positions distributed over one rotor revolution. The tail rotor trim solution for each set of the perturbed states enables the removal of tail rotor states from the computed linear model. Because the rotorcraft motion equation has a fully implicit form as per Eq. (19), the resultant state equations are described with time-varying coefficients as follows:

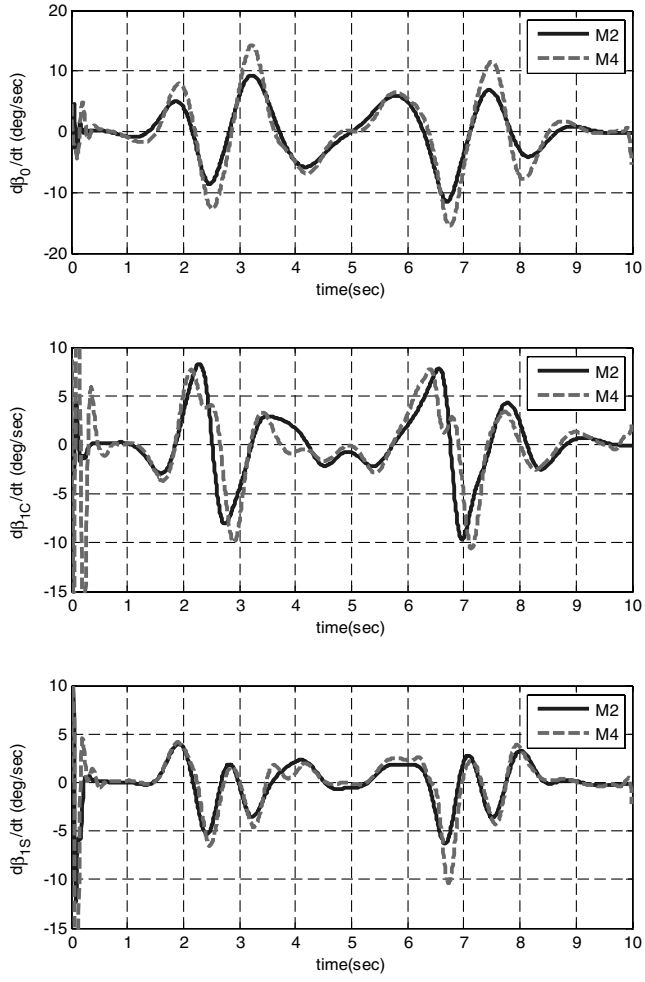

Fig. 16 Time history of flap angular rate for slalom maneuver (NS1500-NI6).

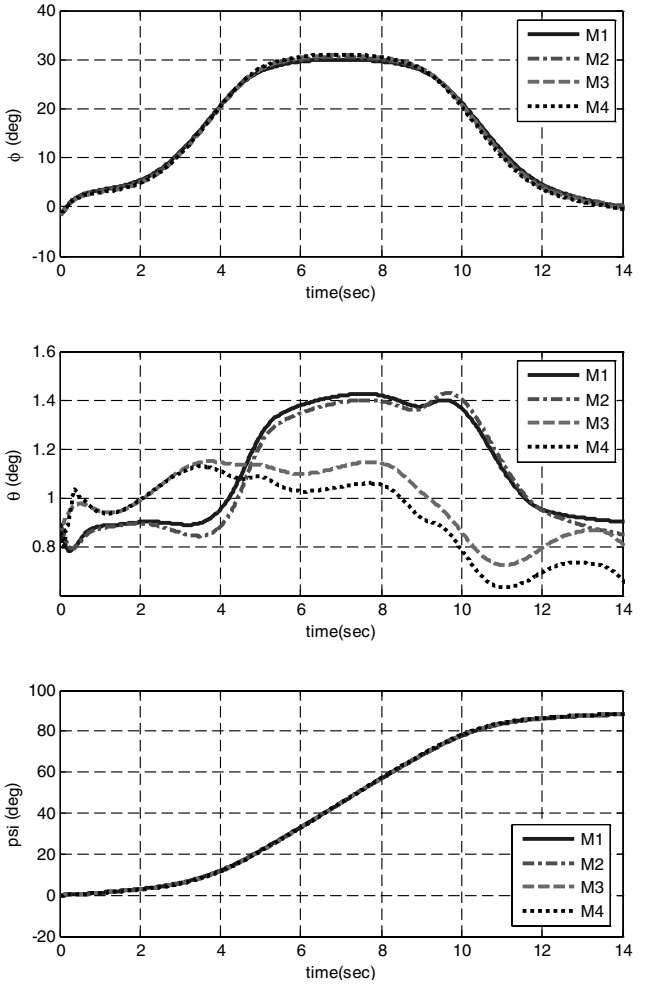

Fig. 17 Time history of attitude and heading angle for turn maneuver (NS1500-NI6).

$$M(t)\dot{x} + K(t)x + C(t)u = 0$$
$$\text{where } M(t) = \left.\frac{\partial f}{\partial \dot{x}}\right|_{\text{trim}},\ K(t) = \left.\frac{\partial f}{\partial x}\right|_{\text{trim}},\ C(t) = \left.\frac{\partial f}{\partial u}\right|_{\text{trim}} \tag{26}$$

The time invariant form of the state equations can be obtained by averaging the matrices $M(t), K(t), C(t)$ over one rotor revolution. The helicopter models developed for this study are categorized per the following identification codes:

1) M1: 6-DOF linear model (only rigid-body DOF)

2) M2: 12-DOF linear model (rigid body, dynamic inflow, and flap DOF)

3) M3: 6-DOF nonlinear model (only rigid-body DOF with main rotor trim)

4) M4: 12-DOF nonlinear model (rigid body, dynamic inflow, and flap DOF)

The states and controls for the 12-DOF model, M4, are defined with the states for rigid body, dynamic inflow, main rotor flap, and controls as

$$\begin{aligned} x &= [x_R, x_I, x_F]^T \qquad x_R = [u, v, w, p, q, r, \phi, \theta, \psi, x_E, y_N, h]^T \\ x_I &= [\lambda_0, \lambda_{1C}, \lambda_{1S}]^T \qquad x_F = [\dot{\beta}_0, \dot{\beta}_{1C}, \dot{\beta}_{1S}, \beta_0, \beta_{1C}, \beta_{1S}]^T \end{aligned} \tag{27}$$

$$u = [\delta_0, \delta_{1C}, \delta_{1S}, \delta_{\text{TR}}]^T \tag{28}$$

The dynamic characters of different models are compared with the characteristic roots of each model in Table 3. The eigenvalues of models M2 and M4 are corresponding to the first and second columns, respectively, and present frequency modes of rotor motion, which are important for maintaining the required model fidelity in the analyses of aggressive maneuvers. The last two columns present those for models M3 and M1, respectively.

V. Applications

The mathematical models outlined in the previous section were applied to study several representative rotorcraft maneuvers, such as bob up, turn, and slalom, for the Bo-105 helicopter configuration. The bob-up maneuver is initiated from hover, whereas the turn and slalom maneuvers begin from a steady level flight at a forward speed of 60 kt. The number of time-integration nodes can be selected to control the time-step size or to improve the accuracy of time integration. Unless otherwise noted, the impulsive start method, in which state and costate variables over all shooting nodes are initialized with the same trim state values, were used. The costate variables are simply set to zero, except the ones corresponding to the cost function, which were set to 1.0. For clarity, the analysis conditions are classified according to the coding convention of Mx-NSy-NIz, which differentiates the chosen mathematical model, number of shooting nodes, and number of integration nodes, in the order of Mx, NSy, and NIz. That is, the notation M4-NS1500-NI6 defines an analysis condition with the nonlinear 12-DOF model, 1500 multiple-shooting nodes, and six time-integration nodes.

Figures 4–6 serve to show how each mathematical model fared in tracing the prescribed trajectories. The different models resulted in a nearly identical trajectory, and the calculated trajectories matched the prescribed paths well, except the heading rate for the turn maneuver. The application of a penalty function for both the heading angle and heading rate deviation is theoretically arguable; however, such an implementation was found to improve numerical stability in practice.

The characteristics of the optimal control solution with MSM were studied with variations in the number of shooting nodes and time-integration stages. For this purpose, the 6-DOF linear model (M1) was used because it enables the rapid attainment of robust solutions during the initial stages of software development. Figure 7 presents the convergence history when MSM is implemented to the bob-up maneuver with a varying number of shooting nodes at the M1-I6 analysis condition. A remarkable reduction in the number of iterations for convergence was found to occur when the number of shooting nodes was increased. In actuality, no convergence was possible when implemented with less than 40 shooting nodes. A similar trial revealed the minimum number of shooting nodes required for the numerical convergence for different models, when the MSM was applied to an unstable system like helicopters. Figure 8 shows the convergence history at the M1-NS50 analysis condition with a varying number of integration nodes, displaying the dependency of numerical convergence on the desired level of time-integration accuracy. Because the total number of time-integration stages is proportional to the product of the number of shooting nodes and the number of integration nodes, a tradeoff between these two parameters is necessary in ensuring both fast convergence and numerical efficiency. Figure 9 differentiates the convergence histories with different methods of initializing state and costate variables at the multiple-shooting nodes. Generally, the convergence speed of MSM is very slow at the early iterative stages because of poor initial guesses. Once the calculated trajectory approaches the converged optimum, then the tolerance for absolute error begins to decrease rapidly. Performing optimal calculations with the results from the M1 model as the initial guesses to the state and costate variables was found to give accelerated convergence for the same analysis with the M3 model. This approach was also discovered to be effective in improving the numerical convergence of the applications with nonlinear models. Even though an impulsive start with the M3 model fails to converge, a converged solution was able to be found when the optimal control calculation results from the M1 or M2 model was used as the initial guesses for the M3 model.

Figures 10–12 present the optimal control solutions for the bob-up maneuver with different models. The computations were performed at the analysis condition of NS1500-NI6. The trim controls and states

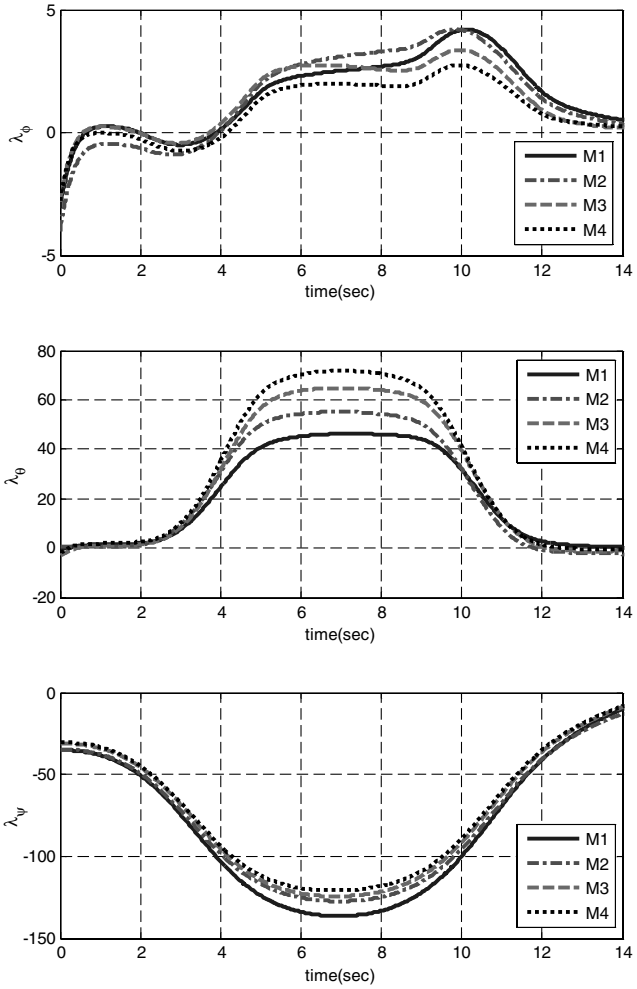

Fig. 18 Time history of costates corresponding to attitude and heading angle (bob-up maneuver, NS1500-NI6).

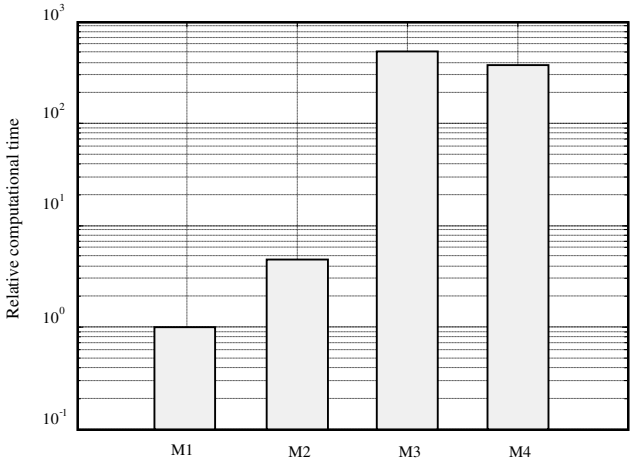

Fig. 19 Relative computational time for one step of MSM iteration with reference to model M1 (bob-up maneuver, NS1500-N16).

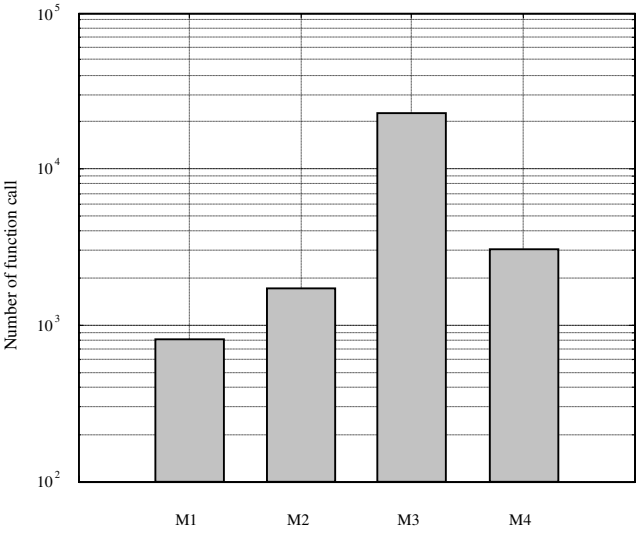

Fig. 20 Number of function calls with reference to that of standard forward simulation (bob-up maneuver, NS1500-NI6).

are added to those calculated by using the linear models M1 and M2 to show a direct comparison between the analysis results with linear and nonlinear models. Depending on the types of model used, the results show noticeable differences in the calculated controls, states, and costate variables. Figures 13 and 14 show the calculated results for the slalom maneuver with the same analysis condition as the bob-up maneuver analyses. As it can be seen, only the roll and heading angles show good correspondence. Figures 15 and 16 present the angles and angular rates of the tip path plane tilt. The flap angles for model M3 were calculated from the main rotor trim solution. The flap responses show an oscillatory behavior before maneuver entry ($t_{\text{entry}} = 1.0$ s) but the succeeding responses are stabilized quickly enough to reach reasonable optimal control solutions. In this study, the trim solutions were obtained by using the fully implicit mathematical model of [21], and the calculated trim conditions were used as the initial conditions for the optimal control problem with model M4. Even small amounts of error in defining an initial steady flight condition can cause this kind of oscillatory behavior, also adversely impacting numerical convergence. Figure 17 is a comparison of the attitude and heading angles calculated for turn maneuvers, and Fig. 18 shows the corresponding costate variables.

Figure 19 compares the relative computational resources required for one iterative step of the MSM at the analysis condition of NS1500-NI6. Here, model M1 is the reference, clocked at 45 s, most of which was spent on calculating the Jacobean matrix M of $F(Z_1, Z_2, \ldots, Z_{m-1})$. The presented analyses were executed on a personal computer with Intel Core2 Quad CPU 2.66 GHz and Intel (R) Fortran Compiler Integration version 9.1 without any OpenMP options. Relative to M1, the required computational times were around 4.5, 517, and 390 times longer for models M2, M3, and M4, respectively. The results show the optimal control approach of rotorcraft maneuver analysis is computationally expensive even with high-end personal computers. Figure 20 presents the ratio of the number of function calls for one iterative step of the MSM. The ratio is defined as the total number of function calls divided by the number of function calls required for a standard forward simulation. The ratios with different models were measured around 830 for M1, 1796 for M2, 23,994 for M3, and 3152 for M4. With the analysis condition of NS1500-NI6, the step size between two adjacent integration nodes corresponded to $\Delta\psi = 2.83$ deg and that between two adjacent shooting nodes corresponded to around $\Delta\psi = 17$ deg. Even though the linear models M1 and M2 reached converged solutions with shooting node numbers of 50 to 60, the nonlinear model M4 required over 1500 shooting nodes for its converged solution with the impulsive start method. Figure 21 shows how the number of shooting nodes affects the optimal control solutions of the slalom maneuver with the M3 model. In the case when fewer than 600 shooting nodes were used, the numerical analysis failed to converge completely. But once converged, the analysis results showed the same trends regardless of the number of shooting nodes used.

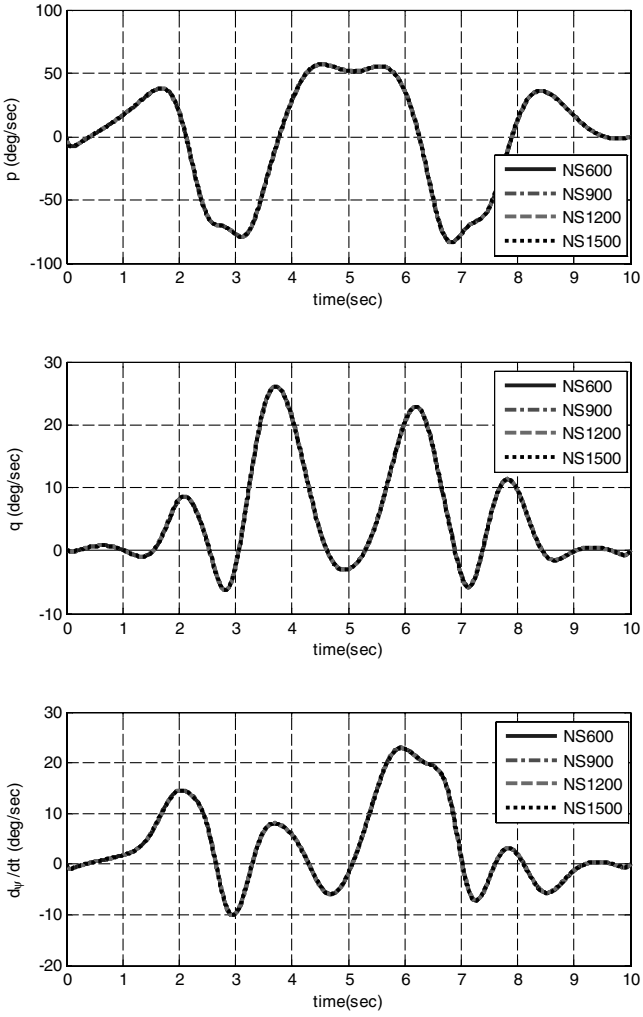

Fig. 21 Effect of the number of shooting nodes on the optimal solution (slalom maneuver, M3-NI6).

VI. Conclusions

A comprehensive study on the model-selection aspect of implementing nonlinear optimal control problems was completed using a helicopter trajectory tracing problem as its scope of research. The numerical results of analyzing different rotorcraft maneuvers

showed that the choice of mathematical model had little impact on optimally predicting the prescribed trajectory. However, there exist large discrepancies in the estimation of other states, costates, and optimal controls, depending on the fidelity level of mathematical models. Also, the convergence behavior towards system optimality was found to strongly depend on model fidelity as well as the number of shooting nodes used for the multiple-shooting method. The inclusion of more accurate rotor modeling equations resulted in a dramatic increase in both the required number of function calls and wait time.

Although the present study exclusively used the indirect method for the maneuver analyses of helicopters, the results can be generalized to provide realistic estimates of required computational resources for implementing optimal control strategies to rotorcraft flight dynamic problems, depending on the desired level of model fidelity. The multilayered modeling approach allows us to research the dependency of 1) the optimal control solution's quality, and 2) the computational efficiency on model fidelity. Furthermore, such a mixed use of low- and high-fidelity models provides a reliable means of checking the validity of the optimal solutions using a low-fidelity model. If proven useful, the strategy is envisioned to motivate an increased utilization of variable fidelity simulation environments, resulting in enhanced numerical stability and computational efficiency when high-fidelity analysis tools are desired to be used for some or all portions of an optimal rotorcraft control problem.

Acknowledgment

This study has been supported by the Korea Aerospace Research Institute (KARI) under the Korean Helicopter Program (KHP) Dual-Use Core Components Development Program funded by the Ministry of Commerce, Industry, and Energy (MOCIE).

References

[1] "Aeronautical Design Standard, Performance Specification, Handling Qualities Requirements for Military Rotorcraft," U.S. Army Aviation and Missile Command, ADS 33E-PRF, Mar. 2000, pp. 25–48.

[2] "Advisory Circular 29-2C; Certification of Transport Category Rotorcraft," Federal Aviation Administration, U.S. Dept. of Transportation, Dec. 2003.

[3] Hess, R. A., and Gao, C., "A Generalized Algorithm for Inverse Simulation Applied to Helicopter Maneuvering Flight," *Journal of the American Helicopter Society*, Vol. 38, No. 3, Oct. 1993, pp. 3–15.

[4] Avanzini, G., and Matteis, G., "Two-Timescale Inverse Simulation of a Helicopter Model," *Journal of Guidance, Control, and Dynamics*, Vol. 24, No. 2, Mar.–Apr. 2001, pp. 330–339.

[5] Celi, R., "Optimization-Based Inverse Simulation of a Helicopter Slalom Maneuver," *Journal of Guidance, Control, and Dynamics*, Vol. 23, No. 2, Mar.–Apr. 2000, pp. 289–297.

[6] Rutherford, S., and Thomson, D. G., "Improved Methodology for Inverse Simulation," *Aeronautical Journal*, Vol. 100, No. 993, Mar. 1996, pp. 79–86.

[7] Bradley, R., and Thomson, D. G., "The Use of Inverse Simulation for Preliminary Assessment of Helicopter Handling Qualities," *Aeronautical Journal*, Vol. 101, No. 1007, Sept. 1997, pp. 287–294.

[8] Cervantes, L., and Biegler, L. T., "Optimization Strategies for Dynamic Systems," *Encyclopedia of Optimization*, Vol. 4, edited by C. Floudas, and P. Pardalos, Kluwer Academic, Norwell, MA, 2001, pp. 216–227.

[9] Bottasso, C. L., Croce, A., Leonello, D., and Riviello, L., "Rotorcraft Trajectory Optimization with Realizability Considerations," *Journal of Aerospace Engineering*, Vol. 18, No. 3, July 2005, pp. 146–155. doi:10.1061/(ASCE)0893-1321(2005)18:3(146)

[10] Sim, Y. C., Leng, S. B., and Subramaniam, V., "A Combined Genetic Algorithms-Shooting Method Approach to Solving Optimal Control Problems," *International Journal of Systems Science*, Vol. 31, No. 1, Jan. 2000, pp. 83–89. doi:10.1080/002077200291488

[11] Betts, J. T., "Survey of Numerical Methods for Trajectory Optimization," *Journal of Guidance, Control, and Dynamics*, Vol. 20, No. 2, Mar.–Apr. 1998, pp. 193–207.

[12] Fraser-Andrews, G., "A Multiple-Shooting Technique for Optimal Control," *Journal of Optimization Theory and Applications*, Vol. 102, No. 2, Aug. 1999, pp. 299–313. doi:10.1023/A:1021728407151

[13] Oberle, H. J., and Grimm, W., "BNDSCO; A Program for the Numerical Solution of Optimal Control Problems," German Aerospace Center, Rept. 515, Oberpfaffenhofen, Germany, 1989.

[14] Grimm, W., and Markl, A., "Adjoint Estimation from a Direct Multiple Shooting Method," *Journal of Optimization Theory and Applications*, Vol. 92, No. 2, Feb. 1997, pp. 263–283. doi:10.1023/A:1022650928786

[15] Padfield, G. D., *Helicopter Flight Dynamics*, Blackwell Science, Boston, MA, 1996, pp. 87–91.

[16] Bottasso, C. L., Chang, C.-S., Croce, A., Leonello, D., and Riviello, L., "Adaptive Planning and Tracking of Trajectories for the Simulation of Maneuvers with Multibody Models," *Computer Methods in Applied Mechanics and Engineering*, Vol. 195, Nos. 50–51, 2006, pp. 7052–7072. doi:10.1016/j.cma.2005.03.011

[17] Bottasso, C. L., Croce, A., Leonello, D., and Riviello, L., "Unsteady Trim of Maneuvering Rotorcraft with Comprehensive Models," Dipartimento Ingegneria Aerospazialem Politechico di Milano Rept. 05-02, Milan, 2005.

[18] Bogdanov, A. A., and Wan, E. A., "Model Predictive Neural Control of a High-Fidelity Helicopter Model," AIAA Paper 2001-4164, 2001.

[19] Kim, C.-J., "Numerical Stability Investigation of Integration Inverse Simulation Method for the Analysis of Helicopter Flight During Aggressive Maneuver," *Spring Meeting of Korean Society for Aeronautical and Space Sciences*, Korean Society for Aeronautical and Space Sciences, Apr. 2002, pp. 201–205.

[20] Kim, C.-J., Jung, S.-N., Lee, J., Byun, Y. H., and Yu, Y. H., "Analysis of Helicopter Mission Task Elements by Using Nonlinear Optimal Control Method," *33rd European Rotorcraft Forum* [CD-ROM], Sept. 2007.

[21] Kim, C.-J., Yun, C. Y., and Choi, S., "Fully Implicit Formulation and Its Solution for Rotor Dynamics by Using Differential Algebraic Equation (DAE) Solver and Partial Periodic Trimming Algorithm (PPTA)," *31st European Rotorcraft Forum* [CD-ROM], Sept. 2005.

[22] Celi, R., "Solution of Rotary-Wing Aeromechanical Problems with Differential-Algebraic Equation Solvers," *Journal of the American Helicopter Society*, Vol. 45, No. 4, Oct. 2000, pp. 253–262.

[23] Bryson, A. E., Jr., and Ho, Y. C., *Applied Optimal Control*, Hemisphere, New York, 1975.

[24] Kirk, D. E., *Optimal Control Theory: An Introduction*, Dover, New York, 1970.

[25] Bonnans, J. F., and Guilbaud, T., "Using Logarithmic Penalties in the Shooting Algorithm for Optimal Control Problems," *Optimal Control Applications and Methods*, Vol. 24, No. 5, 2003, pp. 257–278. doi:10.1002/oca.730

[26] Thomson, D. G., and Bradley, R., "Mathematical Definition of Helicopter Maneuvers," *Journal of the American Helicopter Society*, Vol. 42, No. 4, Oct. 1997, pp. 307–309.

[27] Holsapple, R., Venkataraman, R., and Doman, D., "A Modified Simple Shooting Method for Solving Two Point Boundary Value Problems," *Proceedings of the IEEE Aerospace Conference*, Vol. 6, Inst. of Electrical and Electronics Engineers, Piscataway, NJ, Mar. 2003, pp. 2783–2790.

[28] Chen, R. T. N., "Effects of Primary Rotor Parameters on Flapping Dynamics," NASA TP-1431, 1980.